Analysis of Three Phase Fault Condition & Sharing Power at Different Loads by a Proposed Hybrid AC-DC Smart Micro-Grid

Raja Rashidul Hasan, Member, IEB, Rubel Mahmud, Abedul Hadi, Sujan Howlader

***Abstract*-- This paper proposes a hybrid AC-DC smart micro grid that will electrify rural area by using renewable energy sources. In this proposed hybrid grid system, both AC and DC micro grids are connected through bidirectional converters. In a micro grid system, different loads and distributed generators are connected. In AC side, AC sources and loads are connected. And in DC side DC sources and loads are connected. For stabilize the system under various generation, load and fault condition as well as ensure power sharing among ac, dc and utility grid, different algorithms are proposed. This proposed hybrid grid has been designed and simulated using Simulink in MATLAB. Simulation results show the system remains stable under uncertain change in load, generation and ability to get over from three phase fault operation.**

.

***Index Term*-- PV system, wind, hybrid micro-grid, grid control, three phase fault**

I. INTRODUCTION

Electric distribution technology changes day by day, many changes are becoming remarkable which will fulfill the necessities of energy delivery system. These modifications are being driven both from demand side where higher energy availability and also efficiency are expected. One the other hand from the supply side where the integration of distributed generation and peak savings technologies must be adapted [1]. Due to an increasing amount of distributed energy resources and deregulation, power systems currently undergo considerable change in operating system requirements.

Now a day's distributed energy resources include different technologies which accept generation in micro sources and some of them take advantage of renewable energy resources like solar, wind. Micro sources close to the load has an advantage of reducing transmission losses as well as prevent network fulfillments. The energy storage systems usually include batteries and flywheels [2].

The storing device in micro grid is same to the rotating reverse of large generations in the common grid that confirms the balance between energy generation and consumption especially during fast changes in load or generation [3].From the customer point of view, micro grids offer both thermal and electricity requirements and in addition improve local reliability, reduce emissions, improve power excellence by supportive voltage and reducing voltage dips and potentially lower costs of energy supply. From the utility viewpoint, distributed generation situated close to loads will reduce flows in transmission and distribution circuits with two important effects. These effects are loss reduction and ability to potentially alternative for network assets. Micro grid can also allow network support during the time of stress by relieving congestions and support recuperation after faults. The advancement of micro-grids can contribute to the reduction of emissions and also the migration of climate changes. This is due to the availability and developing technologies for distributed generation units are based on renewable sources and micro sources which are defined by very low emissions [4]. Micro grids offer various advantages to end consumer such as improved energy efficiency, minimized over all energy consumption, reduce greenhouse gases, improved service and quality and reliability and cost efficient electricity in fracture replacement [2].

II. HYBRID SMART MICRO-GRID

Micro-grids are modern, small scale versions of the centralized electricity system. Smart micro-grid generate, distribute and also regulate the flow of electricity locally to the consumers. This is an ideal way to integrate renewable sources and allow for customer participation in the electricity enterprise. Depending on locally available resources, hybrid smart micro grid system can be developed [5]. The most significant environmental benefit of a smart micro-grid is its ability to use local generation and the resulting waste heat to displace coal-fired generation. The smart micro-grid can reuse the energy that is produced during electricity generation. Smart micro-grid also makes it possible to get the most from clean, renewable energy because they have the flexibility needed to use a wider range of energy sources, including those that present a challenge for the current centralized system such as wind and solar [6].

III. MODELING OF THE SYSTEM

A. Proposed smart micro-grid:

The configuration of the proposed hybrid micro grid system shown in Fig. 1, where various kinds of AC sources such as DFIG wind turbine, diesel generator and AC loads can be connected to the AC micro grid. Andvarious kinds of DC sources such as PV array, fuel cell as well as DC loads can be connected to the DC micro grid. AC and DC sides are connected together

through bidirectional converter. The AC bus of the hybrid grid is tied to the utility grid

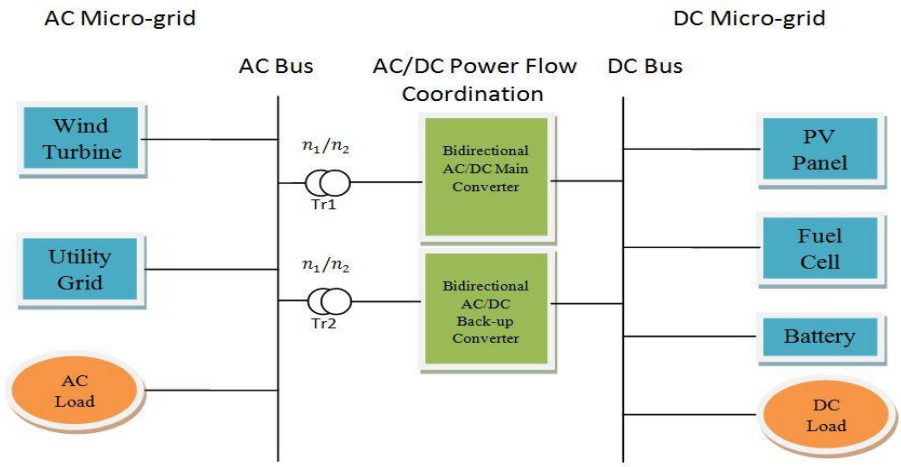

Fig. 1. Proposed Hybrid AC/DC MicroGgrid system

Fig. 2 and Fig. 3 are the Simulink (MATLAB) model of the hybrid micro grid. Fig. 2 is used for analysis uncertain change in load, generation and Fig. 3 is used for analysis three phase fault condition. In DC micro grid a 100kW PV array and 50kW fuel cell is used as DC source. Here boost converter is used to connect PV arrays and fuel cell to the DC micro grid. Variable DC loads are also connected to the DC micro grid. In AC micro grida5MW doubly fed induction generator (DFIG) wind turbine is connected in order to simulate AC sources and Variable AC loads are connected to the AC micro grid for simulating loads. The AC and DC micro grid are coupled through bidirectional converter in order to exchange power. And utility grid is connected to the utility grid through a transformer.

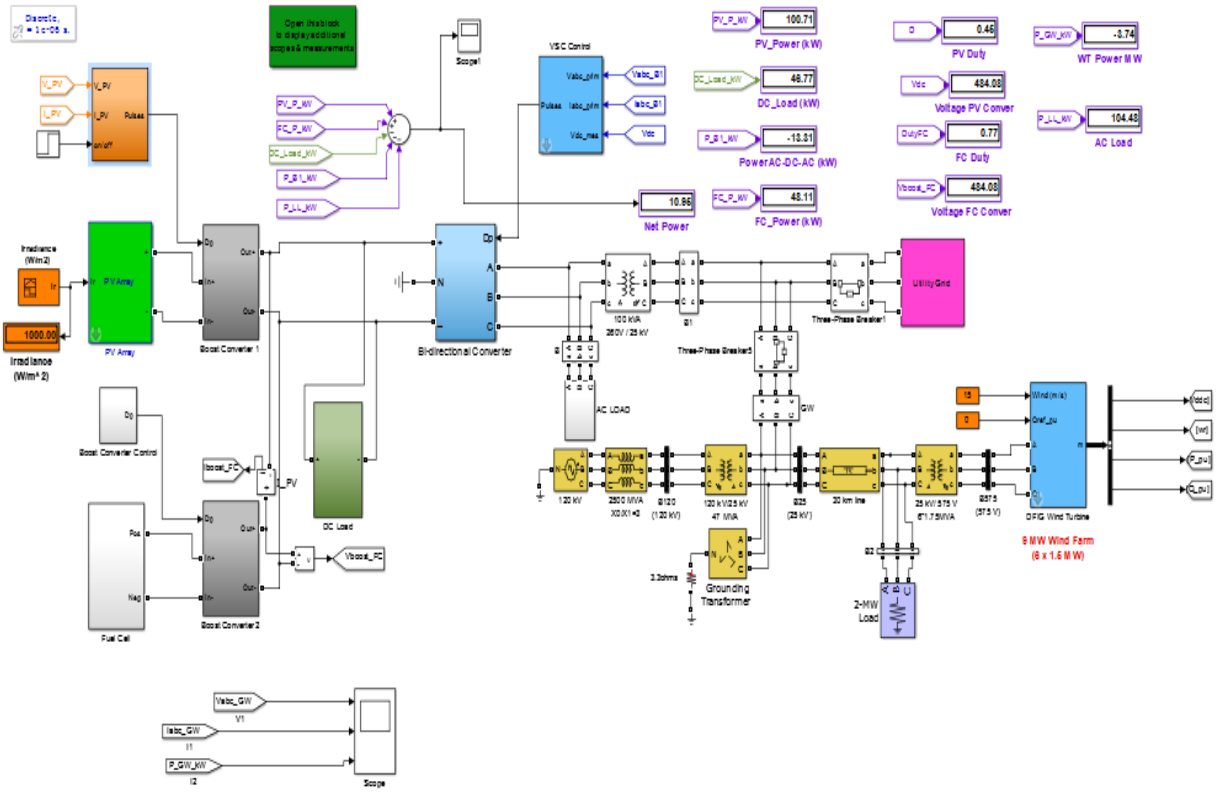

Fig. 2. Simulink (MATLAB) model of Hybrid Micro-Grid

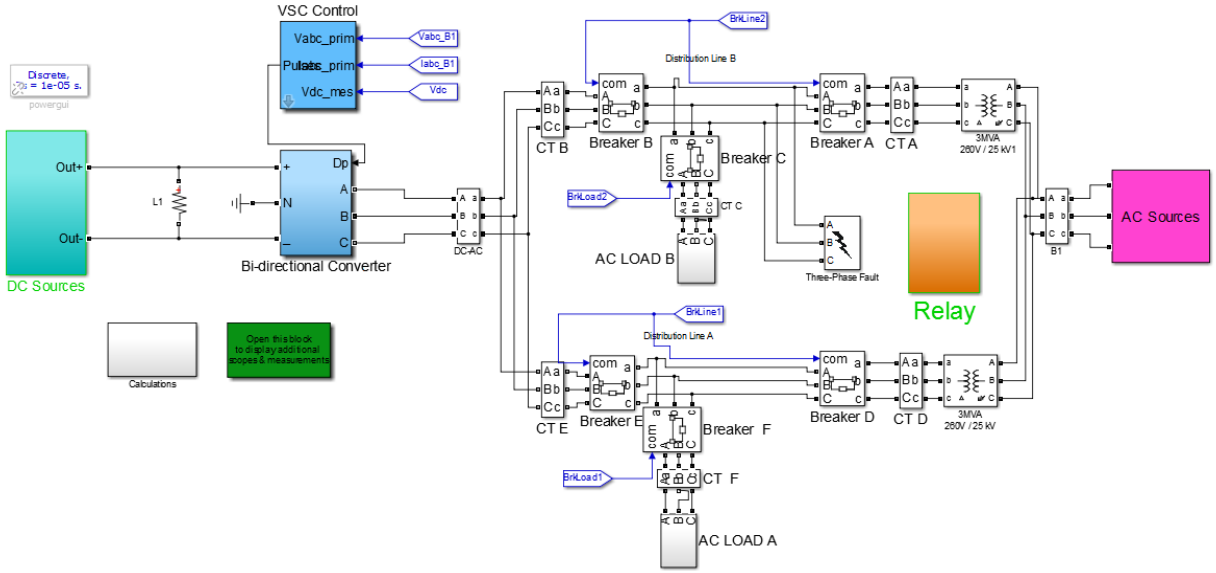

Fig. 3. Model of Fault analysis by Simulink (MATLAB)

B. Operation of grid

The hybrid micro grid performs its operations in two ways. In grid tied mode the bidirectional (VSC) converter provides stable DC bus voltage as well as synchronizes the AC bus voltage with utility grid in this mode. It also exchanges power between AC and DC buses. When output power of DC sources is greater than DC loads this converter reacts like inverter and on this condition power flows from AC to DC side. When generation of total power is less than the total load at DC side, the converter injects power from AC to DC side. This converter The hybrid micro grid performs its operations in two ways. In grid tied mode the bidirectional (VSC) converter provides stable DC bus voltage as well as synchronizes the AC bus voltage with utility grid in this mode. It also exchanges power between AC and DC buses. When output power of DC sources is greater than DC loads this converter reacts like inverter and on this condition power flows from AC to DC side. When generation of total power is less than the total load at DC side, the converter injects power from AC to DC side. This converter helps to receive power from the utility grid incase the total power generation is less than the total load in the hybrid micro grid. Otherwise hybrid grid injects power to the utility grid. Battery role is not important as the power is balanced by utility grid [7].

In autonomous mode the battery can play a very important role for balance voltage stability [7]. In this thesis voltage stability has been ensured only by controlling loads rather than using battery. This means voltage will be stable only if total load is less than total generation. It helps to receive power from the utility grid incase the total power generation is less than the total load in the hybrid micro grid. Otherwise hybrid grid injects power to the utility grid. Battery role is not important as the power is balanced by utility grid [7].

In autonomous mode the battery can play a very important role for balance voltage stability [7]. In this thesis voltage stability has been ensured only by controlling loads rather than using battery. This means voltage will be stable only if total load is less than total generation.

C. PV Panel Model

As PV cells generate low voltage,several PV cells need to connect in series (for high voltage) and parallel (for high current) to form a PV module to get desire output. In practical, to meet the requirement of commercial applications several modules are connected to form array. In Fig. 4 the equivalent circuit diagram consists of a photoncurrent,a diode,a series resistor,a parallel resistor.

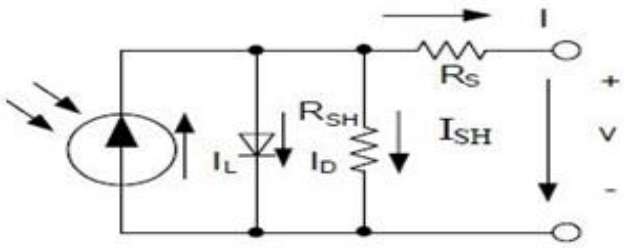

Fig. 4. Equivalent solar cell diagram [8].

So, the equation of the solar cell,

$$I_{pv}=I_{ph}-I_D=I_{ph}-I_0(e^{q(v+IR_s)/AKT_C}-1)-(v+IR_S/R_{Sh}) \quad (1)$$

The photon current,

$$I_{Ph}=[I_{sec}+K_1(Tc-T_R).SI/1000] \quad (2)$$

The shunt resistance is much bigger than load resistance whereas the series resistance is much smaller than a load resistance. So, power losses internally within the cell. So, ignoring two resistances,

$$I_{pv}=I_{ph}-I_D=I_{ph}-I_0(e^{qv/AKT_c}-1) \quad (3)$$

Where, K is Boltzmann's gas constant (1.38×10^{-23} J/K), T_c is Absolute temperature of the cell (K), q is

Electron charge (1.602×10^{-19} J/V), I_o is Saturation current, v is Voltage of PV module, A is Ideal factor, $T_R$is Cell's reference temperature and S.I is Solar Irradiance.

D. PEM Fuel Cell Model

The equivalent circuit diagram is shown in Fig.5. The output voltage of a single fuel cell is defined by Nernst equation and ohm's law [9],

$$V_{fc} = E_{ner} - V_{act} - V_{ohm} - V_{con} \quad (4)$$

And, by solving the equation (4), we get

$$V_{fc} = 1.229 + \times RT/2F[ln(P_{H2}) + ln(P_{O2})] - Aln(i_{cd}) - i_{cd}Ra - me^{(ni_{cd})} \quad (5)$$

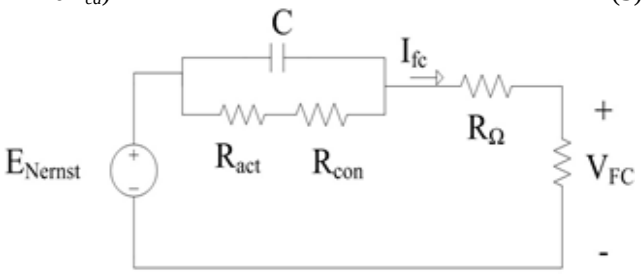

Fig. 5. Equivalent model of PEM fuel cell. [9]

Where, Ener is the voltage of the cell in open circuit, Vact is voltage drop when anode and cathode are active, Vohm is ohmic voltage drop, Vcon is the voltage drop resulting from the reduction in concentration of the reactants gases or from the transport of mass of hydrogen and oxygen, F is Faraday's constant (96485C), R is the universal gas constant (8.314J/K.mol), T is the temperature in Kelvin, P_{H2} and P_{O2} both are partial pressure of Hydrogen and Oxygen respectively in bar, i_{cd} is the cell current density (A/m^2), A is constant, R_a is the area-specific resistance, the values of m is 3×10^{-5} V and n is 8×10^{-3} Cm^2/mA[9],[10].

E. Wind Turbine Generator Model

The equation of power that captured by wind turbine blade,

$$P_{air} = \tfrac{1}{2}[\rho A C_p(\lambda,\beta).V^3 \quad (6)$$

Where, ρ is air density, *A* is the area perpendicular to the air flow, $Cp(\lambda,\beta)$ is the power coefficient, which is the function of tip ratio λ and pitch angle β and V is the speed of wind [11].

The mathematical model of DFIG in state space is needed for control system. The voltage equation in matrix form for a rotational d-q coordinates as follows[11],

$$\begin{bmatrix} V_{ds} \\ V_{qs} \\ V_{dr} \\ V_{qr} \end{bmatrix} = \begin{bmatrix} -R_s & 0 & 0 & 0 \\ 0 & -R_s & 0 & 0 \\ 0 & 0 & R_r & 0 \\ 0 & 0 & 0 & R_r \end{bmatrix} \begin{bmatrix} i_{ds} \\ i_{qs} \\ i_{dr} \\ i_{qr} \end{bmatrix} + p \begin{bmatrix} \lambda_{ds} \\ \lambda_{qs} \\ \lambda_{dr} \\ \lambda_{qr} \end{bmatrix} + \begin{bmatrix} -\omega_a\lambda_{ds} \\ \omega_a\lambda_{qs} \\ -\omega_b\lambda_{dr} \\ \omega_b\lambda_{qr} \end{bmatrix} \quad (7)$$

$$\begin{bmatrix} \lambda_{ds} \\ \lambda_{qs} \\ \lambda_{dr} \\ \lambda_{qr} \end{bmatrix} = \begin{bmatrix} -L_s & 0 & L_m & 0 \\ 0 & -L_s & 0 & L_m \\ -L_m & 0 & L_r & 0 \\ 0 & -L_m & 0 & L_r \end{bmatrix} \begin{bmatrix} i_{ds} \\ i_{qs} \\ i_{dr} \\ i_{qr} \end{bmatrix} \quad (8)$$

At synchronous speed the rotor cannot move and as a result there is no query of induced emf and current, hence there is zero torque, but any speed other than synchronous speed the machine will experience torque which is the case of mirror, where as in case of generator electrical torque in terms of mechanical is provided by means of prime mover that is wind in this case [12].

$$j/n \times dwr/dt = Tm - Ts \quad (9)$$

$$Tm = nLm(iqsidr - ids\ idr) \quad (10)$$

Where, T_m is mechanical torque, T_s is electromagnetic torque, L_m, L_r, L_s are mutual, rotor and stator inductance respectively, j is rotor inertia constant, n is number of pole, ω_a and ω_b are angular synchronous speed and slip speed respectively. Subscripts s and r represents stator and rotor of d and q axis.

If the synchronous rotation d-q reference is oriented by the stator voltage vector, d axis is lined up with stator voltage and q axis with stator flux reference. So, λ_{ds}=0 and λ_{qs}= s [11].

$$ids = -(Lm/Ls).idr$$

$$Te = n.(Lm/Ls).\lambda sidr$$

$$K = LsLr - L2m/LsLr \quad (11)$$

$$Vdr = Rridr + KLr\,(didr/dt) - (\omega s - \omega r)(Lmiqs + Lriqr) \quad (12)$$

$$Vqr = Rridr + KLr\,(didr/dt) + (\omega s - \omega r)(Lmids + Lridr) \quad (13)$$

IV. COORDINATION CONTROL OF THE SYSTEM

There are five converters in this system which have to be coordinately controlled for uninterrupted operation of the system. Again there are six Current Transformers (CT) and six Circuit Breakers (CB). These CTs have to use for control those CBs to protect the system from three phase faults in ac micro-grid. The control algorithms for those converters and CBs are presented in this section.

A. Control of the converters:

The objective of control the boost converter of PV array is to achieve MPPT of PV array by regulating duty cycle of boost converter. Incremental Conductance (IC) method regulates the duty cycle of boost converter to track the MPPT of PV array. IC method which is used in this thesis to control the boost converter of PV is based on IC algorithm described in literature [13].

The control objective of boost converter for FC is to extract maximum power from FC. To achieve this a fixed duty cycle is selected by simulating and observing results for different duty cycle. This fixed duty cycle is 0.67.

One of control objectives of the back to back ac/dc/ac converter of DFIG is to regulate rotor side current to synchronize ac grid and the other objective is to achieve MPPT. In this paper direct torque control (DTC) scheme is used as the control method for the rotor side converter of DFIG. The DTC scheme is described in literature [14].

The objectives of the bi-directional converter controller are to keep a stable dc micro-grid voltage for variable dc loads and to synchronize the ac micro-grid with utility grid. The control scheme for the bi-directional converter used in this paper is based on basic principles described in [15].

B. Control of the circuit breakers (CB):

The control objective of circuit breakers is to protect the system from different three phase faults in ac micro-grid. The position of the CBs and current transformers (CT) are shown in Fig. 6. Here A, B, C, D, E and F are the position of both CT and CB A, B, C, D, E and F respectively. And I_a, I_b, I_c, I_d, I_e, and I_f are current measurements of CT A, B, C, D, E, and F respectively.

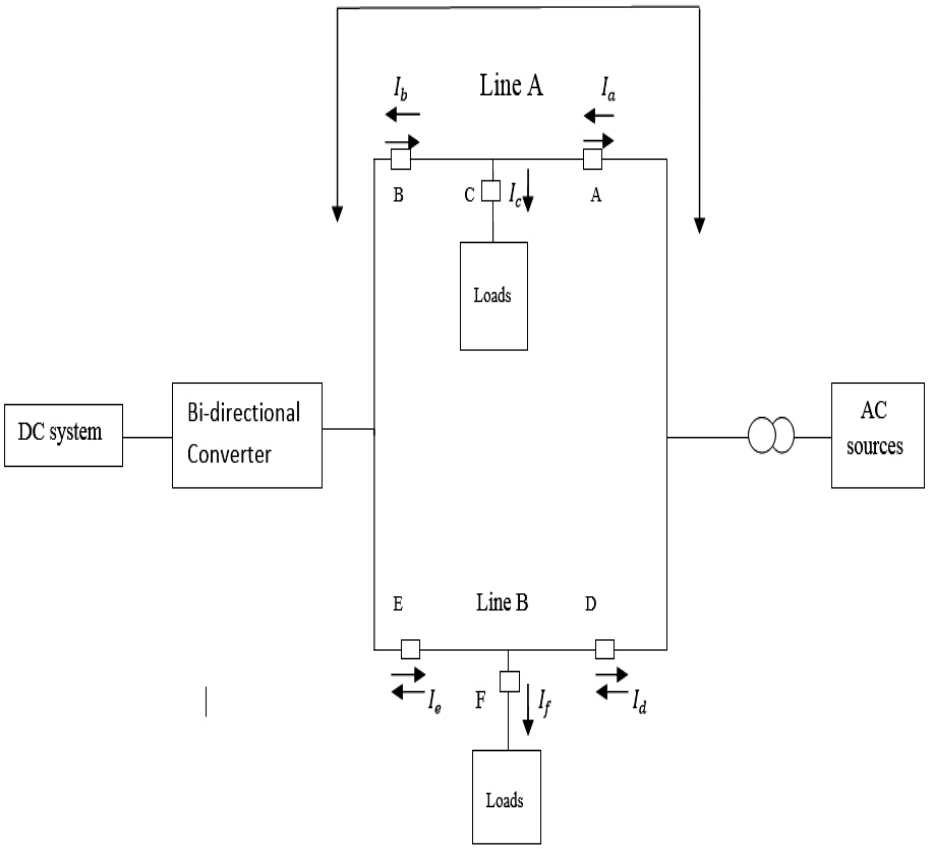

Fig. 6.Single line diagram of hybrid system.

The control algorithm of CB is shown in Fig. 7. In Fig. 7, K is the over load current limit for loads in line A shown in Fig. 6, L is the differential current limit in line A and B shown in Fig. 6, again M is the over load current limit for loads in line B, L is the differential current limit in line A.

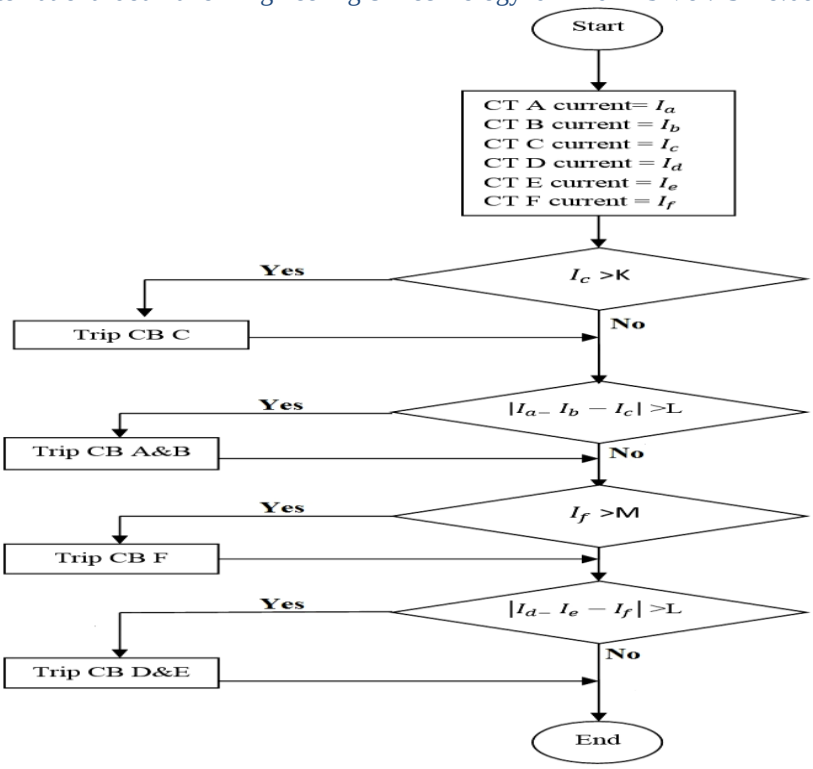

Fig. 7. Control algorithm of circuit breakers.

V. SIMULATION RESULTS

The operations of the hybrid grid are simulated under uncertain change in source and load conditions. The grid tied mode as well as the autonomous mode is simulated by isolating utility grid from the system using circuit breakers. Three phase fault at AC micro grid are also created and removed to verify the proposed model and algorithms.

A. Uncertain change in load and source:

When utility grid is connected with the system then power is balanced by utility grid. There is no need of battery in this mode. But at autonomous mode it is important to keep loads less then sources power. Battery can help to improve the power balance in autonomous mode. In this paper, power is balanced at autonomous mode by controlling loads. System operates in grid tied mode from 0 sec. to 2.7 sec. and rest of the time it operates in autonomous mode.

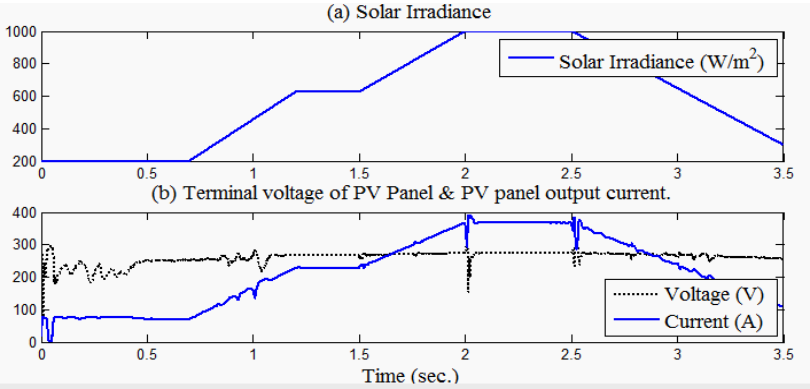

Fig. 8. (a) Solar irradiance (b) Terminal voltage of PV panel and PV panel output current.

In this paper Incremental Conductance(IC) algorithm is used for MPPT of PV based on the corresponding solar irradiation. The solar irradiance is shown in Fig. 8(a) and Fig. 8 (b) shows PV panel terminal voltage and output current response. The terminal voltage is about 260 volt and it has some transient response from 0-0.4 sec. because within this time PV system was at off MPPT mode. Some other transient response of both voltage and current can be seen at 1 sec., 1.5 sec., 2 sec. etc. because of sudden change in loads and or system configuration. It can be

seen that the output current varies to follow the solar irradiance and to achieve maximum power. The terminal voltage and output current of FC are shown in Fig. 9.

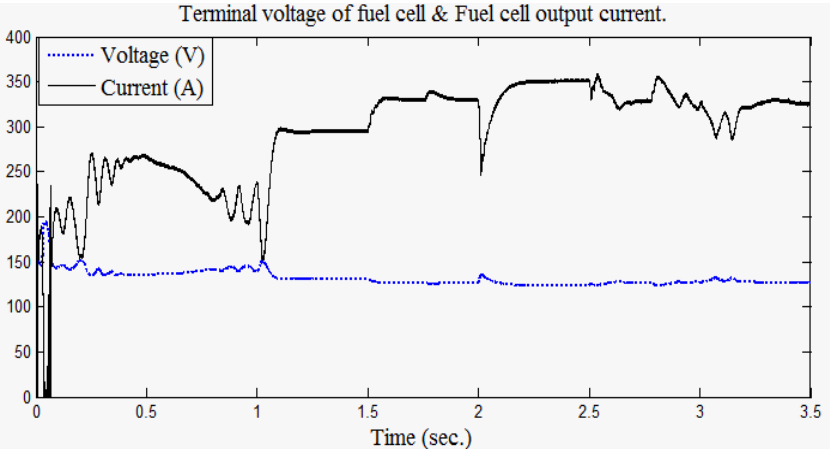

Fig. 9. Terminal voltage of fuel cell and fuel cell output current.

The solar irradiation (radiation level times 1/5 for comparison) and PV output power are shown in Fig. 10(a). The maximum output power of PV array is 100kW for 1000 W/m2 solar irradiation. The initial duty cycle for the IC algorithm is set at 0.5 for 0 sec. to 0.4 sec. The algorithm starts to find new duty cycle after 0.4 sec. and so PV output reaches its maximum for corresponding irradiance after 0.4 sec. Fig. 10(b) shows the FC output which is about 40-45 kW. Fig. 10(c) shows the WT output which is about 4-5 MW. The WT output is zero from 1 sec. to 2.5 sec. because within this time WT was disconnected from the system to check the system response for a huge generation change. Again WT output decreased to less than 700 kW after 2.7 sec.to rest of the time because within this time utility grid was disconnected from system and system goes to autonomous mode. At autonomous mode WT supply power only to the loads. There is several transient responses in Fig. 10 1 sec., 1.5 sec., 2 sec. 2.5 sec. etc. because of sudden change in loads and or system configuration.

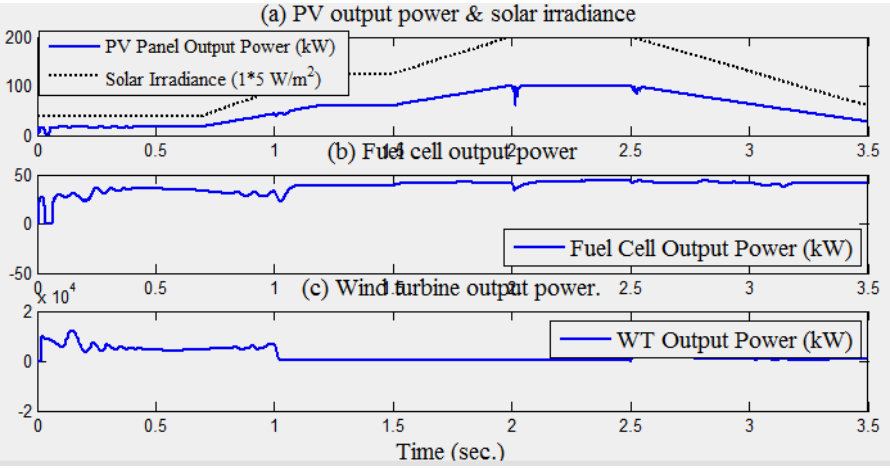

Fig. 10. (a) Solar irradiance (radiation level times 1/5 for comparison) Versus PV output power (b) Fuel cell output power (c) Wind turbine output power.

Fig. 11(a) shows the DC generation versus load variation.Fig. 11(b) Shows power sharing between AC and DC micro-grid. In Fig. 11(b) from 1 sec. to2.7 sec. the curve is in positive y region shows the amount of power which is being shared from DC micro-grid to AC micro-grid. On the other hand from 0 sec. to 1 sec. and 2.7 sec. to 3.5 sec. the curve is in negative y region shows the amount of power being shared from AC micro-grid to DC micro-grid. In Fig. 11(a) at 2.3 sec. the dc generation is 144kW and dc load is 30 kW. At that time Fig. 11(b) shows the value +113, which represents that, at that time ac micro-grid receiving 113 kW power from dc micro grid. On the other hand at 0.6 sec. Fig. 11(a) shows the dc generation is 53kW and dc load is 185 kW. At the same time Fig. 11(b) shows the value -132, which represents that, at that time ac micro-grid injecting 132 kW power to dc micro grid.

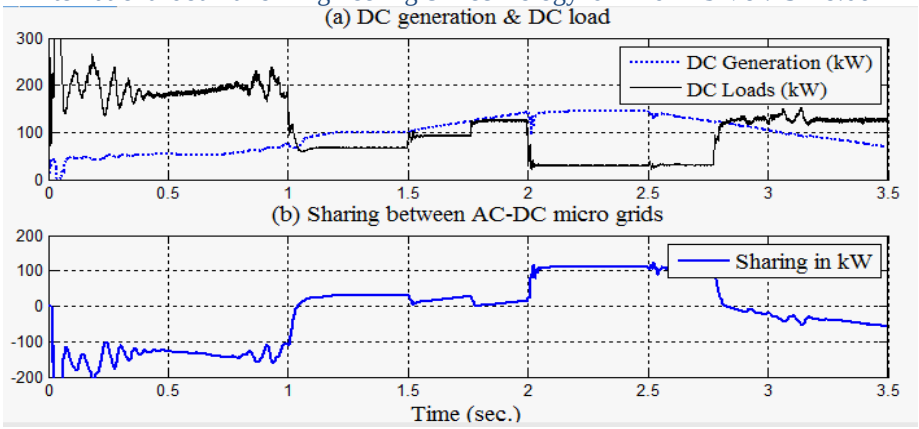

Fig. 11. (a) DC generation versus DC load (b) Sharing between AC-DC micro grids.

Fig. 12(a) shows the total generation versus load variation.Fig. 12(c) Shows power sharing between hybrid grid and utility grid. In Fig 12(c) from 0 sec. to 1 sec. and 2.5 sec. 2.7 sec. the curve is in positive y region shows the amount of power which is being injected to the utility grid by hybrid grid. On the other hand from 1 sec to 2.5 sec. the curve is in negative y region shows the amount of power being shared from utility grid to hybrid grid. From 2.7 sec. to 3.5 sec. the curve remain zero because at this time utility grid is disconnected from system and system is operating in autonomous mode.

At autonomous mode there is no power exchange between utility and hybrid grid. In Fig. 12(a) at 0.6 sec. total generation is 4.23 MW and total load is 1.52 MW. At that time Fig. 12(c) shows the value +2730 which represents that, at that time utility grid is receiving 2.73MW power from hybrid grid. On the other hand at 1.3 sec. Fig. 12(a) shows the total generation is 100 kW , total load is 1432 kW or 1.43 MW and Fig. 12(c) shows the value -1398, which represents that, at that time1398 kW 0r1.39MW power is being shared from utility grid to the hybrid grid.

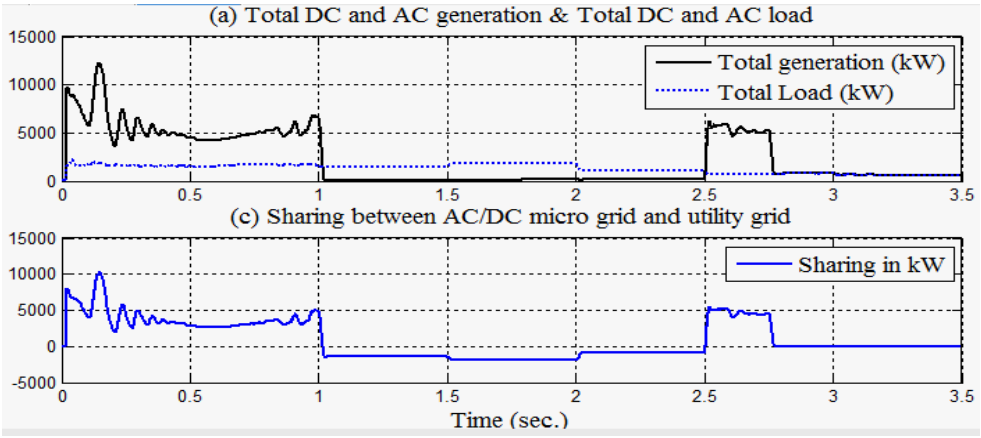

Fig. 12. (a) Total DC and AC generation versus total DC and AC load (c) Sharing between AC/DC micro grid and utility grid.

Fig. 13 shows the AC micro-grid RMS voltage which is about 200- 210 Volt and the DC bus voltage. DC micro-grid voltage which is about 400 Volt. Both voltage have transient response because of load or system configuration change. But it can be seen that DC bus voltage is more sensitive than AC bus voltage.

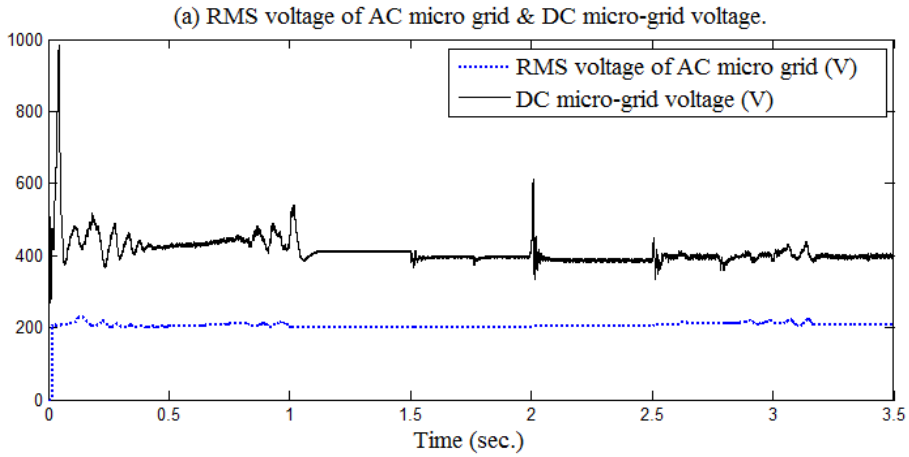

Fig. 13. Transient response of DC bus voltage and AC bus RMS voltage.

Fig. 14 shows the AC Phase a voltage of utility grid and AC micro-grid. By comparing AC quantities it can be seen that AC micro-grid has a constant 13 degree phase difference from utility grid and both of them have same frequency of 60 Hz.

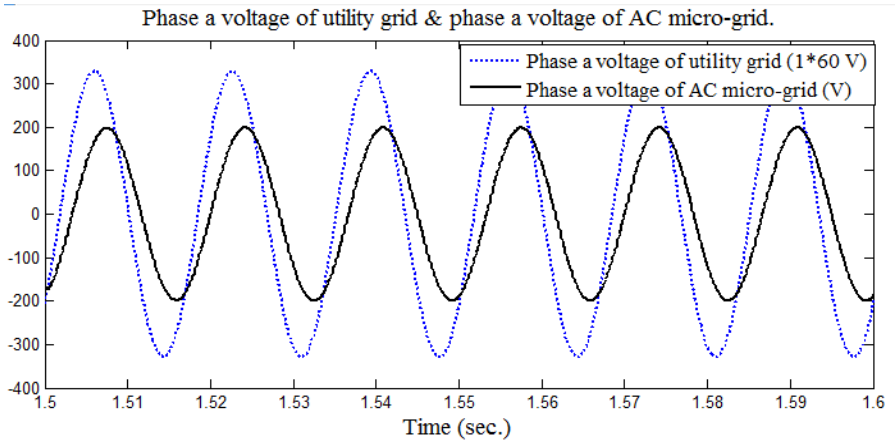

Fig. 14. Phase a voltage of utility grid (Voltage level times 1/60 for comparison) versus Phase a voltage of AC micro-grid

B. Three phase fault in AC micro grid:

The single line diagram of AC micro grid is shown in Fig. 6 which has been used for three phase fault analysis. To perform fault analysis AC micro-grid is split into two parallel distribution lines named “Line A” and “Line B”. A three phase fault is identified using differential relay for both “Line A” as well as “Line B” and using O/C relay for AC loads.

Different three phase fault are created in “Line A” at 0.7 sec. The relay and CBs isolate “Line A” at 0.9 sec. For a single line to ground fault the three phase fault voltages of “Line A” and “Line B” is shown in Fig. 15(a) and Fig. 15(b) respectively. The DC micro-grid voltage is shown in Fig 15(c).

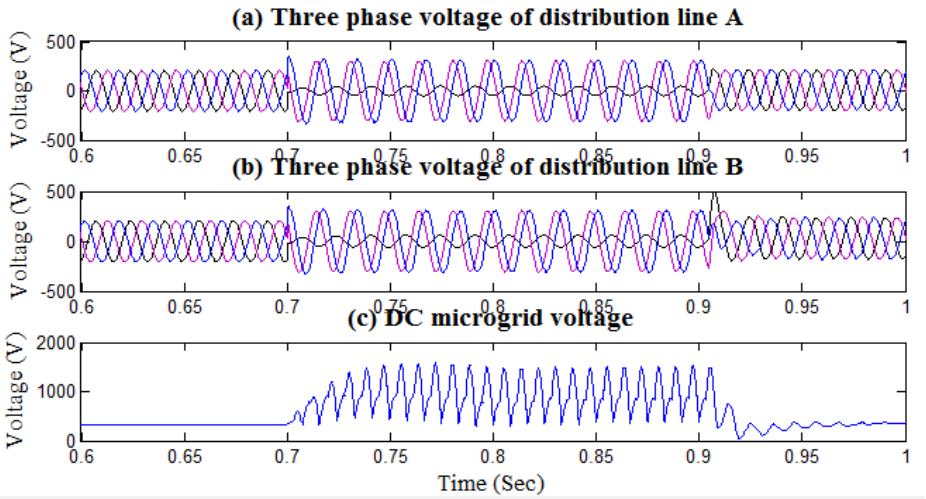

Fig. 15. (a) Three phase voltage of distribution "Line A" (b) Three phase voltage of distribution "Line B" (c) DC voltage level of DC micro grid.

On the other hand Fig. 16(a) and 16(b) shows the fault currents of "Line A" and "Line B" respectively. The current of "Line A" is zero from 0.9 sec. because at that time "Line A" is disconnected from the system due to remove the fault. It can be seen from Fig.15 and Fig. 16 that the system restores its normal position within 0.01 sec. after a single line to ground fault is removed from the system.

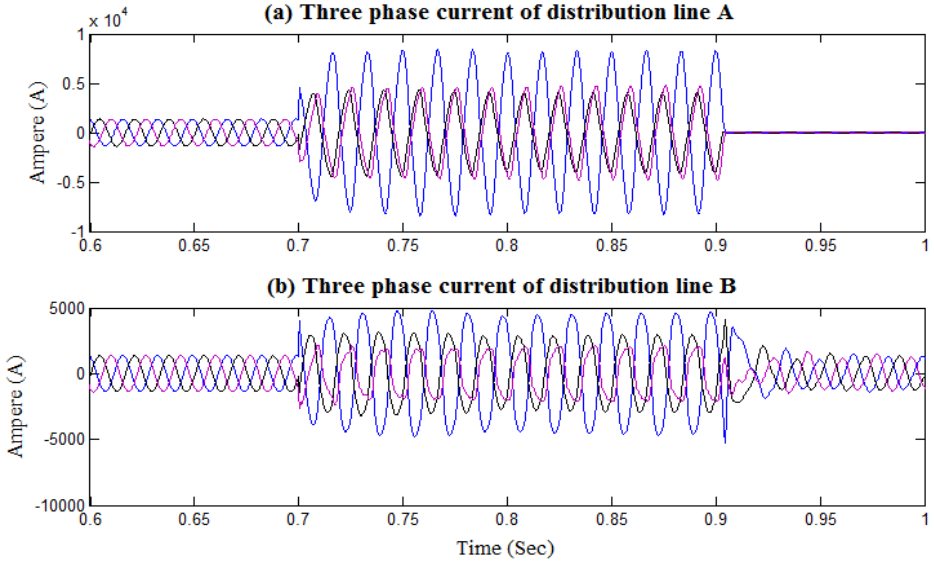

Fig. 16. (a) Three phase current of distribution "Line A" (b) Three phase current of distribution "Line B".

Fig. 17 and 18 are similar to Fig. 15 and 16 respectively with only difference is that a double line to ground fault is observed here. It can be seen from Fig. 17 and Fig. 18 that the system takes 0.18 sec. to restore its normal position after a double line to ground fault is removed from the system. Fig. 19 is similar to Fig. 15 and Fig. 17 with only difference is that a three phase to ground fault is observed here. It can be seen from Fig.19 that the system takes 0.5 sec. to restore its normal position after a three phase to ground fault is removed from the system.

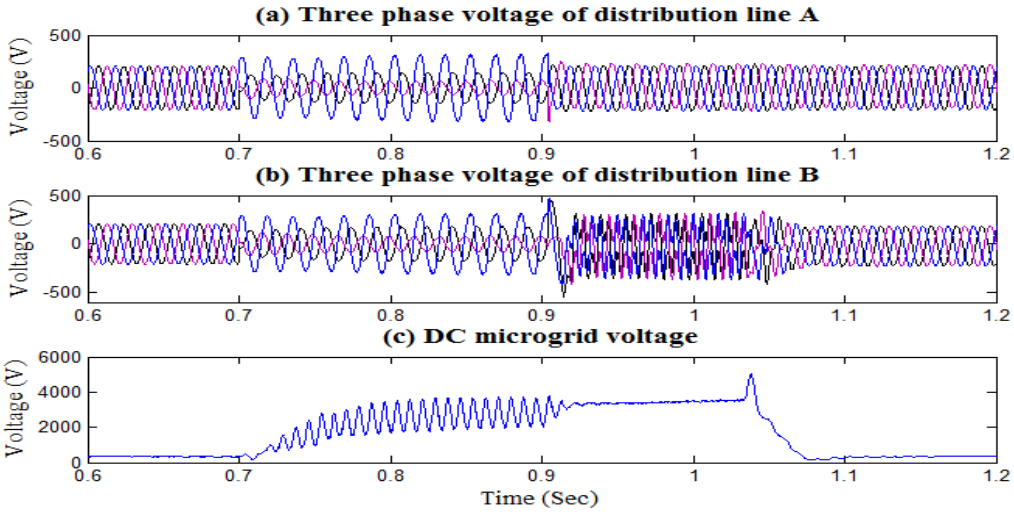

Fig. 17. (a) Three phase voltage of distribution "Line A" (b) Three phase voltage of distribution "Line B" (c) DC voltage level of DC micro grid.

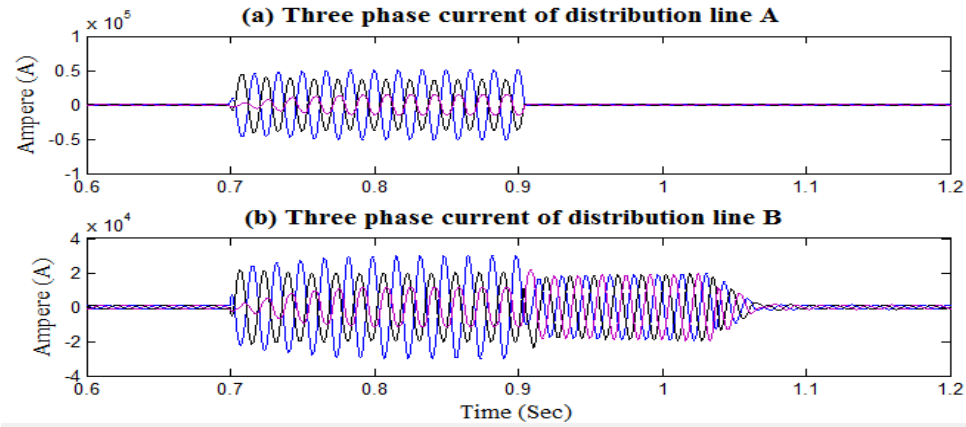

Fig. 18. (a) Three phase current of distribution "Line A" (b) Three phase current of distribution "Line B".

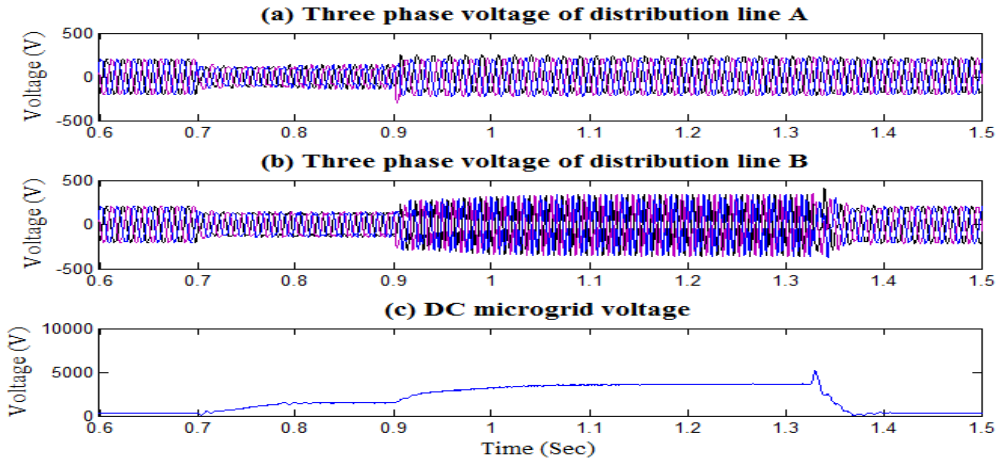

Fig. 19. (a) Three phase voltage of distribution "Line A" (b) Three phase voltage of distribution "Line B" (c) DC voltage level of DC micro grid.

TABLE 1 shows the time that system takes to restore its normal position after removal of a fault. TABLE 2 shows the experimental result of fault current for different kind of faults. Here position "A" and "B" are the positions where measurements are taken. These positions are shown in Fig. 6.

TABLE I

TIME TAKEN FOR RESTORE SYSTEM NORMAL POSITION

Fault Type	Transient Time (sec.)
Single line to ground	0.01
Double line to ground	0.18
Three phase to ground	0.5
Line to line	0.25
Three phase	0.45

TABLE II

EXPERIMANTAL RESULTS OF FAULT CURRENT

Fault Type	Fault current at position "A" Ampere (A)	Fault current at position "B" Ampere (A)
Single line to ground	9000	5600
Double line to ground	20000	35000
Three phase to ground	18000	35000
Line to line	15000	34000
Three phase	18000	35000

It can be seen from Fig. 15 to Fig. 19 and from Table I and II that, the AC micro grid and hybrid grid system can continue its normal operation after remove the fault from the system. For different fault it takes 0.01 to 0.5 sec. to overcome the transient

VI. CONCLUSION

In this thesis the hybrid grid system configuration is done in MATLAB environment. The goal is to accelerate realization of the main benefit to use renewable energy. The hybrid grid may be effective for small isolated industrial plants with PV systems, wind turbine and fuel cell as the major power supply. This power supply system increase energy efficiency and also improves reliability. A hybrid AC-DC smart micro grid system concept may implemented with further expansion to the cellular micro grid system. The protection system of a hybrid AC-DC grid is more critical than traditional grid system. For this lots of work can be done.

REFERENCES

[1] S. Bose, Y. Liu, K. Bahei-Eldin, J.de Bedout, and M. Adamiak, "Tie line Controls in Microgrid Applications," in iREP Symposium Bulk Power System Dynamics and ControlVII, Revitalizing Operational Reliability, pp. 1-9, Aug. 2007.

[2] R. H. Lasseter, "MicroGrids," in Proc. IEEE-PES'02, pp. 305-308, 2002.

[3] Michael Angelo Pedrasa and Ted Spooner, "A Survey of Techniques Used to Control Microgrid Generation and Storage during Island Operation," in AUPEC, 2006.

[4] F. D. Kanellos, A. I. Tsouchnikas, and N. D. Hatziargyriou, "Microgrid Simulation during Grid-Connected and Islanded Mode of Operation," in Int. Conf. Power SystemsTransients (IPST'05), June. 2005.

[5] Potty, K.A, Manipal Inst. of Technol, Manipal Univ., Manipal, India, Keny, P, Nagarajan, C, "An intelligent microgrid with distributed generation," in Innovative SmartGrid Technologies - Asia (ISGT Asia), 2013.

[6] (2015) Blogger website. [Online]. [Cited: January 28, 2015.]Available:http://saikatblog1993.blogspot.com/2015/01/what-is-renewable-energy.html.

[7] V.Madhavi, J.V.R.Vithal,"Modeling and Coordination Control of Hybrid AC/DC" in ISSN 2250-2459, ISO 9001:2008 Certified Journal, Volume 4, Issue 8, August 2014.

[8] Hua Yu, Qiuqin Yue, Jielin Zhou and Wei Wang "A Hybrid Indoor Ambient Light and Vibration Energy Harvester for Wireless Sensor Nodes" in ISSN 1424-8220, pp.8740-8755, 19 May, 2014.

[9] Maria Outeiro and A. Carvalho, "MatLab/Simulink as design tool of PEM Fuel Cells as electrical generation systems", European Fuel Cell Forum, 28 June -1 July 2011.

[10] J. Larminie, A. Dicks, "Fuel cell systems explained", 2nd edition, John Wiley & Sons, England, 2003.

[11] X. Liu, P. Wang and P. C. Loh, "A hybrid AC/DC microgrid and its coordination control", IEEE Trans. Smart Grid, Jun. 2011, 2(2): 278-286.

[12] D.A. Staton, R.P. Deodhar, W.L. Soong, T.J.E. Miller " Torque prediction using the flux-MMF diagram in AC, DC, and reluctance motors ," IEEE Trans. on Industry Application, vol. 32, no. 1, pp. 180- 188 , Jan 1996.

[13] Srushti R. Chafle, Uttam B. Vaidya, "Incremental conductance mppt technique for pv system", ISSN (Print),vol. 2, issue 6, pp. 2320 – 3765, June. 2013

[14] S. Arnalte, J. C. Burgos, and J. L. Rodriguez-amenedo, "Direct torque control of a doubly-fed induction generator for variable speed wind turbines," Elect. Power Compon. Syst., vol. 30, no. 2, pp. 199–216, Feb. 2002.

[15] Y. Sozer and D. A. Torrey, "Modeling and control of utility interactive inverters," IEEE Trans. Power Electron., vol. 24, no. 11, pp. 2475–2483, Nov. 2009.